

Communication Compression for Distributed Learning with Aggregate and Server-Guided Feedback

Tomas Ortega, Chun-Yin Huang, Xiaoxiao Li and Hamid Jafarkhani

Abstract—Distributed learning, particularly Federated Learning (FL), faces a significant bottleneck in the communication cost, particularly the uplink transmission of client-to-server updates, which is often constrained by asymmetric bandwidth limits at the edge. Biased compression techniques are effective in practice, but require error feedback mechanisms to provide theoretical guarantees and to ensure convergence when compression is aggressive. Standard error feedback, however, relies on client-specific control variates, which violates user privacy and is incompatible with stateless clients common in large-scale FL. This paper proposes two novel frameworks that enable biased compression without client-side state or control variates. The first, Compressed Aggregate Feedback (CAF ϵ), uses the globally aggregated update from the previous round as a shared control variate for all clients. The second, Server-Guided Compressed Aggregate Feedback (CAF ϵ -S), extends this idea to scenarios where the server possesses a small private dataset; it generates a server-guided candidate update to be used as a more accurate predictor. We consider Distributed Gradient Descent (DGD) as a representative algorithm and analytically prove CAF ϵ ’s superiority to Distributed Compressed Gradient Descent (DCGD) with biased compression in the non-convex regime with bounded gradient dissimilarity. We further prove that CAF ϵ -S converges to a stationary point, with a rate that improves as the server’s data become more representative. Experimental results in FL scenarios validate the superiority of our approaches over existing compression schemes.

Index Terms—Distributed Learning, Optimization, Federated Learning, Compression, Error Feedback.

I. INTRODUCTION

In distributed learning, a central server coordinates the training of a global model using data distributed across multiple clients. The objective is to minimize a global loss

An early version of this work was submitted to the IEEE International Conference on Acoustics, Speech and Signal Processing (ICASSP), Barcelona, Spain, 2026 [1].

This work was supported in part by the NSF Award ECCS-2207457. Tomas Ortega and Hamid Jafarkhani are with the Center for Pervasive Communications and Computing, University of California, Irvine, CA, USA 92697 (e-mail: {tomaso, hamidj}@uci.edu). Chun-Yin Huang and Xiaoxiao Li are with the Computer Engineering Department at the University of British Columbia, Vancouver, BC, Canada, and Vector Institute, Toronto, ON, Canada (e-mail: {chunyinh, xiaoxiao.li}@ece.ubc.ca).

function f , which is the average of the local loss functions of the clients

$$f(x) = \frac{1}{N} \sum_{n=1}^N f_n(x), \quad (1)$$

where $x \in \mathbb{R}^d$ is the global model, $f_n: \mathbb{R}^d \rightarrow \mathbb{R}$ is the loss function of Client n , and N is the total number of clients. This formulation is prevalent in Federated Learning (FL) [2], a distributed learning paradigm designed for privacy preservation, where clients train the global model on their local data and send updates to the server for aggregation.

A primary bottleneck in distributed learning is communication overhead, especially the cost of uploading model updates from clients to the server [3]. To mitigate this, various lossy compression techniques, such as quantization [4], sparsification [5], and low-rank approximation [6], have been proposed. While unbiased compressors are often easier to analyze, biased compressors are frequently preferred in practice for their superior empirical performance and computational efficiency [3], [7].

To guarantee the convergence of algorithms using biased compression, a mechanism known as error feedback (or error compensation) is typically required [8]. This involves each client tracking the accumulated compression error locally and correcting for it in subsequent updates. However, standard error feedback requires stateful clients to store these error vectors (control variates). In many large-scale, cross-device FL settings, clients are assumed to be stateless and cannot maintain state between communication rounds [3]. Furthermore, having the server manage these control variates on behalf of clients would introduce privacy risks by tracking individual client behavior over time.

This paper addresses these challenges by proposing two novel frameworks that enable biased compression without requiring client-side state or per-client server-side tracking. The core idea is to provide clients with a globally consistent predictor vector. Clients then compress the **difference** between their local update and this predictor. If the predictor is a good approximation of the local update, the difference vector will be sparse or will have a small magnitude, making it highly compressible.

We propose two distinct sources for this predictor, Compressed Aggregate Feedback (CAF ϵ) and Server-Guided Compressed Aggregate Feedback (CAF ϵ -S). The

first, **CAFé**, uses the aggregated and decoded update from the *previous* communication round, Δ_s^{k-1} , as the predictor for the current round k . This approach is entirely self-contained, requires no additional data, and is suitable for any FL setting. Clients receive this shared vector from the server along with the new model, use it for compression, and then discard it, thus remaining stateless. The second framework, **CAFé-S**, is designed for scenarios where the server has access to a small private dataset relevant to the global learning task. The server uses this dataset to compute a “candidate update”, Δ_c^k , which serves as a more timely and potentially more accurate predictor than the lagged aggregate from **CAFé**.

Both frameworks are inspired by the use of temporal prediction in video coding, where compressing the difference between consecutive frames yields significant gains [9]. We analyze both methods in the **Distributed Gradient Descent (DGD)** setting for non-convex objectives. Our theoretical contributions show that **CAFé** improves the convergence rate over standard compressed DGD, while **CAFé-S** achieves a convergence rate that depends on the similarity between the server’s data and the clients’ data. Experimental results on standard FL benchmarks confirm that our proposed methods outperform existing compression schemes.

The remainder of this paper is organized as follows. We review related work in communication compression and error feedback in Section II. We then formally introduce the **CAFé** and **CAFé-S** frameworks in Section III. In Section IV, we provide a detailed convergence analysis for both methods, comparing their theoretical guarantees with the DCGD baseline. Finally, we present our experimental validation in Section V and conclude in Section VI.

II. RELATED WORK

Communication compression is a well-studied topic in distributed learning, and error feedback is often suggested to improve convergence guarantees [10]. In [8], the authors study the error feedback mechanism for one-bit per coordinate biased compression. For general sparse compressors, error feedback was studied in [11], [12]. For the decentralized setting, [13], [14] proposed variants of error feedback with general compression operators. For asynchronous methods, [15], [16] also showed that a modified error feedback with general compression operators has good convergence guarantees. In the non-convex setting, [17] showed that error feedback can be used in arbitrarily heterogeneous settings, which was later extended to the stochastic and convex settings in [7]. All these methods, however, adhere to the traditional model of per-client error accumulation, making them unsuitable for stateless FL environments. Our work departs from this by using a global, shared predictor, eliminating the need for client-specific states.

III. PROPOSED FRAMEWORKS

To discuss the algorithm design, first, we must cover some compression preliminaries. When clients send a mes-

sage to the server, they first encode it using a function E . The server decodes the received information using a function D . We call these functions the encoder and decoder, respectively. For a general compression mechanism, the composition $D(E(x)) := \mathcal{C}(x)$ is called a compression operator [11].

Definition 1. A compression operator is a function $\mathcal{C}: \mathbb{R}^d \rightarrow \mathbb{R}^d$, paired with a positive compression parameter $\omega < 1$, such that for any vector x ,

$$\mathbb{E} [\|\mathcal{C}(x) - x\|^2] \leq \omega \|x\|^2. \quad (2)$$

Example 1 (Top-k compression [4]). The top- k operator zeroes out all but the k largest-magnitude elements of a vector. It satisfies Eq. (2) with $\omega = 1 - k/d$.

Next, we describe how compression operators are used when minimizing the global loss function from Eq. (1) in a distributed learning setting. The fundamental algorithm for this purpose is Distributed Compressed Gradient Descent (DCGD) — see Algorithm 1. The pseudocode shows how, at each round, the global model is sent to the clients, which train it using gradients computed with local data. Clients then compress these gradients and send them to the server, which averages them to update the global model. This process is repeated for any desired number of rounds. Note that DCGD is a specific instance of the

Algorithm 1 Distributed Compressed Gradient Descent (DCGD)

- 1: **Input:** Initial model x^0 , Rounds K , Encoder-Decoder (E, D) pair for compression, learning rate γ
- 2: Initialize global model x^0 , and aggregate $\Delta_s^0 \leftarrow 0$
- 3: **for** round k from 0 to $K - 1$ **do**
- 4: Send x^k to all clients
- 5: **for** each client n in parallel **do**
- 6: $y_n^k \leftarrow x^k - \gamma \nabla f_n(x^k)$ \triangleright Train x^k using local data, store the output in y_n^k
- 7: $\Delta_n^k \leftarrow y_n^k - x^k = -\gamma \nabla f_n(x^k)$ \triangleright Compute local update
- 8: Send $E(\Delta_n^k)$ to server \triangleright Upload local update
- 9: **end for**
- 10: Server decodes each client n via $q_n^k \leftarrow D(E(\Delta_n^k))$
- 11: Server aggregates client updates $\Delta_s^k := \frac{1}{N} \sum q_n^k$
- 12: Server updates model $x^{k+1} := x^k + \Delta_s^k$.
- 13: **end for**

general distributed learning framework, where we have chosen gradient descent as the optimizer for local models, and equal-weight averaging for the aggregation strategy. We can derive a general strategy by not determining the aggregation strategy for client updates, nor the optimizer for on-client training.

A. **CAFé** overview

Our framework, **CAFé**, leverages the previous aggregated update Δ_s^{k-1} to help clients compute a more compressible

update. Namely, clients will compress the difference between their local update Δ_n^k and the previous aggregated update

$$E(\Delta_n^k - \Delta_s^{k-1}).$$

On the server side, the server will add the previous aggregated update when decoding the received messages

$$q_n^k \leftarrow D(E(\Delta_n^k - \Delta_s^{k-1})) + \Delta_s^{k-1}. \quad (3)$$

The pseudocode for this procedure is described in Algorithm 2, where the novelty with respect to the general distributed learning framework is highlighted in green boxes.

Algorithm 2 Compressed Aggregate Feedback (CAFe)

```

1: Input: Initial model  $x^0$ , Rounds  $K$ , Encoder-Decoder
   ( $E, D$ ) pair for compression, learning rate  $\gamma$ 
2: Initialize global model  $x^0$ , and aggregate  $\Delta_s^{-1} \leftarrow 0$ 
3: for round  $k$  from 0 to  $K - 1$  do
4:   Send  $x^k$  and  $\Delta_s^{k-1}$  to all clients ▷ In the
   stateful version  $\Delta_s^{k-1}$  may be omitted
5:   for each client  $n$  in parallel do
6:     Compute local update  $\Delta_n^k \leftarrow -\gamma \nabla f_n(x^k)$ 
7:     Upload difference: send  $E(\Delta_n^k - \Delta_s^{k-1})$  to
   server
8:   end for
9:   Server decodes each client  $n$  via
   
$$q_n^k \leftarrow D(E(\Delta_n^k - \Delta_s^{k-1})) + \Delta_s^{k-1}$$

10:  Server aggregates  $\Delta_s^k := \frac{1}{N} \sum_{n=1}^N q_n^k$ 
11:  Server updates model  $x^{k+1} := x^k + \Delta_s^k$ 
12: end for

```

The intuition is that if the client gradients do not change drastically between rounds, Δ_n^k will be close to the average update Δ_s^{k-1} , making their difference highly compressible.

This method allows for stateless participation, as the predictor Δ_s^{k-1} is provided by the server. However, if a client participated in the previous round and retained the model x^{k-1} , they can locally recover the predictor via $\Delta_s^{k-1} = x^k - x^{k-1}$ without additional communication. Explicit transmission of the predictor is therefore only strictly necessary for clients that are dropping in, returning after absence, or strictly memory-constrained.

In many popular distributed learning algorithms, x^k and x^{k-1} determine Δ_s^{k-1} , like Distributed Gradient Descent, FedAvg, etc. In other words, since the predictor Δ_s^{k-1} represents the net global model update, this framework naturally accommodates server-side momentum or adaptive optimizers (e.g., Adam). In such cases, Δ_s^{k-1} captures the momentum-accumulated velocity, which stabilizes the update trajectory and often serves as a more accurate predictor of the next step than raw gradients alone.

Note that the error feedback mechanism in [17] is a special case of CAFe with a single client. In this case, the aggregated update at the server is simply the client

update, and we can analyze it as a control variate. However, in the multi-client setting, the aggregated update is a combination of all client updates, which acts as a proxy for client-specific control variates and requires novel analysis, shown in Section IV.

B. CAFe-S overview

Our second proposal, CAFe-S, is designed for scenarios where the server holds a small private dataset, with a corresponding loss function $f_s(x)$. Instead of using the lagged update Δ_s^{k-1} , the server computes a candidate update, $\Delta_c^k = -\gamma \nabla f_s(x^k)$, using its own data and the current model x^k . This candidate update is sent to clients as the predictor. The procedure is detailed in Algorithm 3.

Algorithm 3 Server-Guided Compressed Aggregate Feedback (CAFe-S)

```

1: Input: Initial model  $x^0$ , rounds  $K$ , compression
   ( $E, D$ ), learning rate  $\gamma$ , server loss  $f_s$ 
2: for round  $k$  from 0 to  $K - 1$  do
3:   Server computes candidate  $\Delta_c^k \leftarrow -\gamma \nabla f_s(x^k)$ 
4:   Server sends  $x^k$  and  $\Delta_c^k$  to all clients
5:   for each client  $n$  in parallel do
6:     Compute local update  $\Delta_n^k \leftarrow -\gamma \nabla f_n(x^k)$ 
7:     Upload difference: send  $E(\Delta_n^k - \Delta_c^k)$  to server
8:   end for
9:   Server decodes each client  $n$  via
   
$$q_n^k \leftarrow D(E(\Delta_n^k - \Delta_c^k)) + \Delta_c^k$$

10:  Server aggregates  $\Delta_s^k := \frac{1}{N} \sum_{n=1}^N q_n^k$ 
11:  Server updates model  $x^{k+1} := x^k + \Delta_s^k$ 
12: end for

```

If the server's data distribution is similar to the average distribution of clients, Δ_c^k will be a highly accurate predictor of Δ_n^k , leading to even greater compression gains than CAFe.

Remark 2 (Communication Trade-off). *In the stateless configuration, the server must transmit the predictor Δ_s^{k-1} (for CAFe) or Δ_c^k (for CAFe-S) to the clients alongside the global model x^k . While this effectively doubles the downlink payload compared to standard DGD, the trade-off is favorable in Federated Learning for several reasons. First, edge client connections (e.g., LTE/5G, residential broadband) are typically highly asymmetric, with downlink bandwidth significantly exceeding uplink bandwidth [18]. Second, the predictor is a single global vector broadcast to all participants, whereas client updates are unique unicast transmissions. Therefore, maximizing the compression of the scarce unicast uplink capacity at the expense of the abundant broadcast downlink capacity is potentially a net-positive strategy.*

IV. ANALYSIS

Having formally defined both frameworks, we now proceed to analyze their convergence properties. We choose

Gradient Descent as the optimizer for local training, as it is representative of a wide range of distributed learning algorithms [2], [3]. We proceed with the following standard assumptions [3], [10]:

Assumption 1 (L-Smoothness). *The objective function f is L -smooth, which implies that it is differentiable, ∇f is L -Lipschitz, and*

$$f(y) \leq f(x) + \langle \nabla f(x), y - x \rangle + \frac{L}{2} \|y - x\|^2. \quad (4)$$

Also, the objective function f is lower-bounded by f^* .

Assumption 2 (Bounded Local Dissimilarity). *The local gradients have bounded dissimilarity, that is, there exists a $B^2 \geq 1$ such that*

$$\frac{1}{N} \sum_{n=1}^N \|\nabla f_n(x)\|^2 \leq B^2 \|\nabla f(x)\|^2. \quad (5)$$

For reference, we first state the convergence of the baseline DCGD algorithm.

Theorem 1. [DCGD Convergence] *Under Assumptions 1 and 2, with a learning rate $\gamma \leq \frac{1}{L}$ and a compression parameter ω such that $\omega B^2 < 1$, DCGD satisfies*

$$\frac{1}{K} \sum_{k=0}^{K-1} \mathbb{E} \left[\|\nabla f(x^k)\|^2 \right] \leq \frac{2(f(x^0) - f^*)}{\gamma K} \cdot \frac{1}{1 - \omega B^2}. \quad (6)$$

Proof Sketch. The proof relies on a standard descent lemma [19, Section 1.2.3]. The main challenge is to bound the variance introduced by compression, $\mathbb{E} \left[\|\bar{e}^k\|^2 \right]$, which represents the average compression error. Using Assumption 2, we can show this error is bounded by the gradient norm: $\mathbb{E} \left[\|\bar{e}^k\|^2 \right] \leq \omega B^2 \mathbb{E} \left[\|\nabla f(x^k)\|^2 \right]$. Plugging this bound into the descent lemma and telescoping the sum over K iterations yields the final result. The full proof with details is in Appendix B \square

A. Analysis of CAFE

The key benefit of CAFE is that it improves the dependency on the compression parameter ω .

Theorem 2. [CAFE + DGD Convergence] *Under Assumptions 1 and 2, with a learning rate*

$$\gamma \leq \frac{1 - \omega}{L(1 + \omega)} \quad (7)$$

and $\omega B^2 < 1$, CAFE with DGD satisfies

$$\frac{1}{K} \sum_{k=0}^{K-1} \mathbb{E} \left[\|\nabla f(x^k)\|^2 \right] \leq \frac{2(f(x^0) - f^*)}{\gamma K} \cdot \frac{1 - \omega}{1 - \omega B^2}. \quad (8)$$

Proof Sketch. The analysis for CAFE is more involved because the predictor Δ_s^{k-1} creates a temporal dependency: the compression error at Round k is linked to the aggregate update (and thus the error) from Round $k-1$. We cannot bound the error at Step k purely by the state at Step k , as we do for DCGD.

The proof, detailed in Appendix B, proceeds in two main parts. We first derive a bound that links the expected error at Step $k+1$, $\mathbb{E} \left[\|\bar{e}^{k+1}\|^2 \right]$, to the error at Step k , $\mathbb{E} \left[\|\bar{e}^k\|^2 \right]$ and the model gradients. Second, we define a Lyapunov function $\Psi^k := \mathbb{E} \left[f(x^k) + C \|\bar{e}^k\|^2 \right]$ for a carefully chosen constant $C = \frac{\gamma}{2(1-\omega)}$. By combining our recursive error bound with the standard descent lemma, we show that this Lyapunov function decreases at each step ($\Psi^{k+1} \leq \Psi^k - (\text{progress term})$). Telescoping this inequality proves convergence. \square

Comparing Theorem 2 to Theorem 1, CAFE introduces an improvement factor of $(1 - \omega)$. This is significant for aggressive compression where ω is close to 1.

B. Analysis of CAFE-S

The analysis for CAFE-S requires an additional assumption that quantifies the similarity between the server's data and the clients' data.

Assumption 3 (Bounded Server-Client Dissimilarity). *The local gradients and the server gradient have bounded dissimilarity, that is, there exists a $G^2 \geq 0$ such that*

$$\frac{1}{N} \sum_{n=1}^N \|\nabla f_n(x) - \nabla f_s(x)\|^2 \leq G^2 \frac{1}{N} \sum_{n=1}^N \|\nabla f_n(x)\|^2. \quad (9)$$

A small G^2 implies that the server's data is a good proxy for the aggregate client data.

Theorem 3. [CAFE-S + DGD Convergence] *Under Assumptions 1 to 3, with a learning rate $\gamma \leq \frac{1}{L}$, and a compression parameter ω such that $\omega G^2 B^2 < 1$, CAFE-S with DGD satisfies*

$$\frac{1}{K} \sum_{k=0}^{K-1} \mathbb{E} \left[\|\nabla f(x^k)\|^2 \right] \leq \frac{2(f(x^0) - f^*)}{\gamma K (1 - \omega G^2 B^2)}. \quad (10)$$

Proof Sketch. The proof for CAFE-S has a structure very similar to that of DCGD (Theorem 1). The key difference is in how we bound the compression error $\mathbb{E} \left[\|\bar{e}^k\|^2 \right]$.

Instead of compressing the raw update Δ_n^k , clients compress the difference $\Delta_n^k - \Delta_c^k$. We bound the error of this compression using Assumptions 2 and 3, which shows that $\mathbb{E} \left[\|\bar{e}^k\|^2 \right] \leq (\omega G^2 B^2) \mathbb{E} \left[\|\nabla f(x^k)\|^2 \right]$. This error bound has the exact same form as the DCGD bound, but with the factor ωB^2 replaced by the (potentially much smaller) factor $\omega G^2 B^2$. The rest of the proof is identical to that of Theorem 1. The full proof is in Appendix B. \square

Theorem 3 shows that CAFE-S achieves a convergence rate that depends on the similarity between the server's data and the clients' data. This result is intuitive: if the server's data is a perfect match ($G^2 = 0$), the algorithm achieves the same convergence rate as DCGD. For all values of $G^2 < 1$, CAFE-S outperforms DCGD, which reflects the advantage of having a representative dataset at the server.

C. Discussion of the theoretical results

Let us highlight the implications of our theoretical findings. Comparing **CAFé** (Theorem 2) with the baseline **DCGD** (Theorem 1), we observe an improvement factor of $(1 - \omega)$ in the convergence bound for the same learning rate, which becomes significant as compression becomes more aggressive (i.e., as ω approaches 1). This gain comes at the cost of a stricter learning rate condition, $\gamma \leq \frac{1-\omega}{L(1+\omega)}$, which is common for error-feedback methods. In practice, however, we usually chose learning rates much smaller than $\frac{1}{L}$, so this condition is not a significant limitation.

Comparing **CAFé-S** (Theorem 3) with **DCGD** (Theorem 1), we see a different kind of improvement. The convergence rate of **CAFé-S** depends on $1 - \omega G^2 B^2$ instead of $1 - \omega B^2$. The new term G^2 , defined in Assumption 3, quantifies the dissimilarity between the server's gradient and the average of the clients' gradients. If the server's data represent the global data distribution, G^2 will be small ($G^2 < 1$), resulting in a faster convergence rate compared to **DCGD**. In the ideal case where the server's data is a perfect proxy ($G^2 \rightarrow 0$), the negative impact of both compression (ω) and client heterogeneity (B^2) on the convergence rate is eliminated. Importantly, **CAFé-S** achieves this improvement without imposing additional constraints on the learning rate, keeping the standard **DCGD** condition, $\gamma \leq \frac{1}{L}$.

In short, the main take-aways from this analysis are as follows: **CAFé** is a *data-free* method. It provides a *guaranteed* convergence improvement of $(1 - \omega)$ over standard compression, making it desirable for aggressive compression, but it requires a smaller learning rate. In contrast, **CAFé-S** is a *data-dependent* method. It provides a *conditional* improvement if the server's data represent the population (low G^2). It has no learning rate penalty, but its performance depends on the quality of the server-side dataset.

V. EXPERIMENTAL RESULTS

We now empirically validate the theoretical findings of Section IV. Our experiments are designed to: (i) demonstrate the core working principle that our difference-based compression is effective, (ii) compare the end-to-end performance of **CAFé** against baselines with various datasets and compression methods, and (iii) validate the **CAFé-S** hypothesis (Theorem 3) that convergence performance is directly tied to the quality of the server's data. The code to reproduce all experiments is publicly available [20].

A. Experimental Setup

We conducted FL experiments with 10 clients on MNIST [21], EMNIST [22], CIFAR-10 and CIFAR-100 [23] datasets. We used **CONV4** models for MNIST/EMNIST, a **Dense6** model for CIFAR-10, and a **ResNet-20** model for CIFAR-100, following the setup in [24]. We present results for both homogeneous and heterogeneous data cases, denoted *iid* and *non-iid*, respectively. For the latter, we randomly sampled 40% of the total classes for each

client. For each round of communication, which we refer to as a global training round, all clients participated in training. Clients performed one local Gradient Descent training epoch with a batch size of 64 per global training round. We varied the number of global training rounds for each experiment. We ran each experiment with 3 random seeds and report the accuracy means and standard deviations.

The learning rates for each dataset and model combination were tuned by performing a sweep over a set of seven log-spaced candidate values, ranging from 10^{-3} to 10^0 . We selected the rate that yielded the highest accuracy during the specified number of rounds. This process was performed independently for each method (combination of task and compressor), and we found that the optimal rates were approximately consistent across both frameworks. The exact learning rates used in each experiment are tabulated in Tables V and VI. We also provide a detailed sensitivity analysis for the learning rate and further details on the compressor setup in Appendix A.

B. Validation of working principle

The premise of our proposed frameworks is that the difference between the local update and a shared predictor is more compressible than the raw update itself. To quantify this, we define the *Compression Gain Ratio* for a predictor P at Round k as

$$\frac{\|\Delta_n^k - P\|}{\|\Delta_n^k\|}. \quad (11)$$

A ratio smaller than one indicates that the predictor reduces the magnitude of the vector to be compressed.

To visualize this principle, we simulated a Federated Logistic Regression task using synthetic data ($D = 200$, 10 clients, iid data, and a server-side dataset of the same size) over 500 communication rounds, with no compression. We log the updates that would be sent with no modification, with **CAFé**, and with **CAFé-S**. Fig. 1 presents the analysis of the training dynamics and the corresponding logs. The left panel displays the global training loss, confirming that the model converges to the optimum. The middle panel plots the Compression Gain Ratio. During the active training phase, **CAFé** consistently achieves a ratio below 1.0, confirming that the difference vector's magnitude is smaller than that of the raw gradient. We observe that as the model converges and the gradients vanish (approaching Round 500), the ratio trends toward 1.0. This occurs because both the update Δ_n^k and the predictor Δ_s^{k-1} approach zero, and the relative benefit of the predictor diminishes as the updates become dominated by stochastic noise. The right panel shows the log-density histogram of the update values aggregated across the entire training process. The **CAFé** distribution (blue) is significantly narrower compared to the direct updates (red). For clarity, we omit the **CAFé-S** distribution, which closely resembles that of **CAFé**. This increased sparsity suggests that the difference vectors are more efficient to compress.

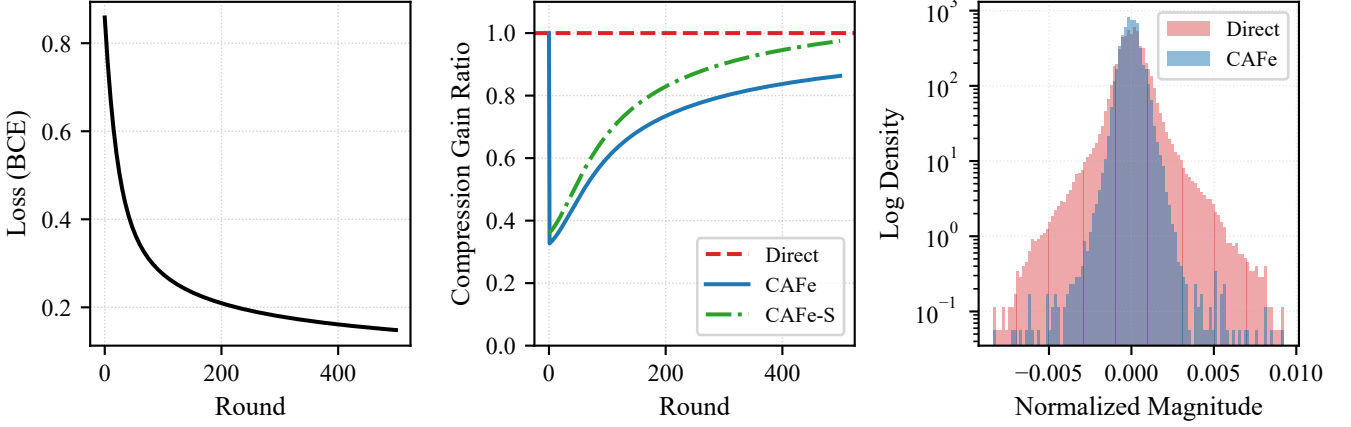


Fig. 1: Analysis of the CAFE working principle on a synthetic logistic regression task. **Left:** Global training loss showing convergence. **Middle:** The Compression Gain Ratio (ρ) remains below 1.0 for the majority of training, indicating that the difference vector has a smaller norm than the raw update. The ratio approaches 1.0 as the model converges. **Right:** The log-density histogram shows that CAFE updates are more peaked at zero (sparser) than direct updates.

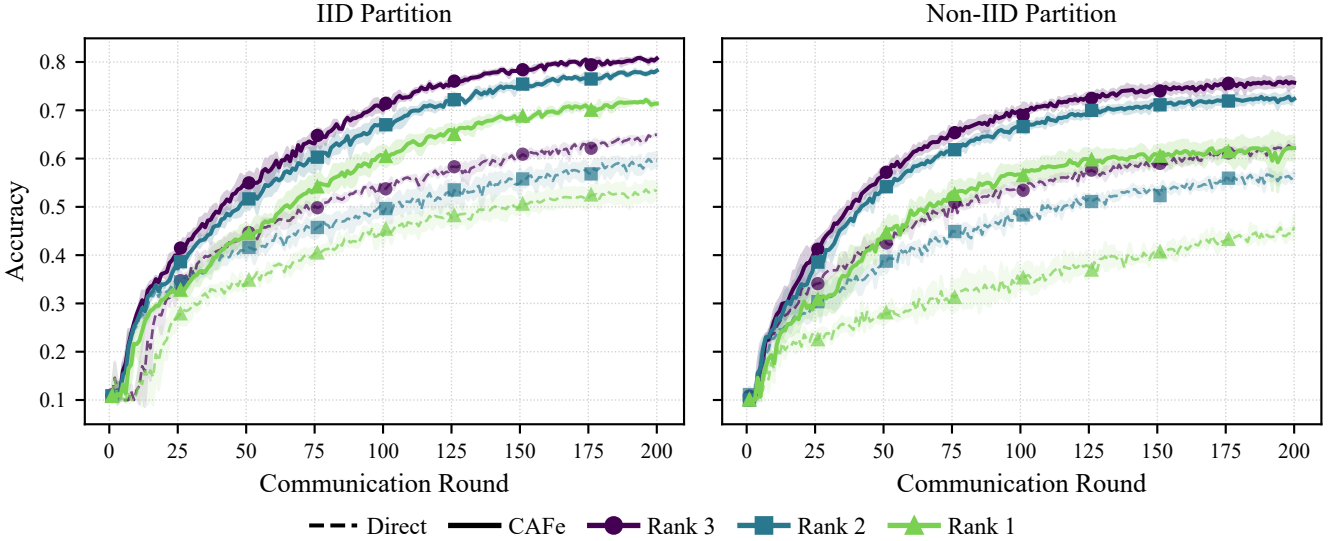


Fig. 2: Learning curves comparing direct compression (Direct) and CAFE with Low-rank compression in the CIFAR-10 task for iid and non-iid settings. CAFE results are presented with solid lines, and Direct compression results are presented with dashed lines. CAFE demonstrates faster convergence and higher accuracy.

C. Performance of CAFE

Having validated the premise, we now evaluate the end-to-end performance of CAFE against direct compression in FL. We test four biased compression methods. First, we use *Top-k* (see Example 1), which retains only the k elements with the largest magnitudes. Second, we use *Low-rank approximation* via PowerSGD [6], which compresses the update matrix by decomposing it into the product of two smaller matrices of rank r (which we vary from 1 to 3), effectively projecting the update onto a lower-dimensional subspace. We also evaluate variants where these compressed outputs are further quantized to lower bit-widths. Sparsification is performed before quantization

since it is optimal for FL [25]. We also include an uncompressed baseline as a reference. The results for various compression parameter settings are reported in Tables I and II. The communication cost in bits per parameter (bpp) for each compression method and parameter setting is reported in Tables III and IV.

The results align with our theory: CAFE consistently outperforms or matches existing direct compression methods. This is particularly stark in aggressive compression settings (low bpp). For instance, in the CIFAR-10 iid task with Top-1% + 4-bit Quantization, Direct compression collapses to random chance (13.0%), whereas CAFE recovers a performance of 72.5%. Similarly, with Rank-1 Low-

TABLE I: Accuracy for CAFE and Direct compression (MNIST, EMNIST).

Compressor	Param.	MNIST (CONV4, 50 rounds)				EMNIST (CONV4, 50 rounds)			
		iid 10 classes/client		non-iid 4 classes/client		iid 47 classes/client		non-iid 4 classes/client	
		Direct	CAFe	Direct	CAFe	Direct	CAFe	Direct	CAFe
None	—	99.3 \pm 0.0		99.0 \pm 0.0		88.9 \pm 0.1		82.2 \pm 0.2	
Top-k	k=10%	99.4 \pm 0.0	99.4 \pm 0.0	99.0 \pm 0.1	99.0 \pm 0.1	88.9 \pm 0.0	88.9 \pm 0.1	81.8 \pm 0.6	81.7 \pm 0.1
	k=1%	99.2 \pm 0.0	99.3 \pm 0.0	98.7 \pm 0.1	98.9 \pm 0.1	88.0 \pm 0.1	88.3 \pm 0.1	79.5 \pm 0.2	81.4 \pm 0.3
	k=0.1%	98.7 \pm 0.1	99.0 \pm 0.1	97.6 \pm 0.3	98.1 \pm 0.1	85.6 \pm 0.3	86.9 \pm 0.2	69.0 \pm 2.3	75.2 \pm 0.2
Top-1% + Quantizer	6 bits	99.3 \pm 0.0	99.2 \pm 0.1	98.7 \pm 0.1	98.9 \pm 0.1	88.1 \pm 0.1	88.3 \pm 0.1	79.7 \pm 0.7	81.3 \pm 0.2
	5 bits	99.3 \pm 0.0	99.3 \pm 0.0	98.6 \pm 0.1	98.9 \pm 0.1	88.2 \pm 0.1	88.5 \pm 0.1	80.6 \pm 0.2	81.7 \pm 0.8
	4 bits	99.3 \pm 0.0	99.2 \pm 0.1	98.5 \pm 0.1	98.8 \pm 0.1	88.0 \pm 0.2	88.4 \pm 0.1	79.1 \pm 0.6	81.2 \pm 0.3
Low-rank	rank=3	99.0 \pm 0.1	99.2 \pm 0.1	98.4 \pm 0.1	98.8 \pm 0.0	86.5 \pm 0.1	88.3 \pm 0.1	74.6 \pm 1.1	79.7 \pm 0.6
	rank=2	98.9 \pm 0.1	99.2 \pm 0.1	98.2 \pm 0.1	98.8 \pm 0.0	85.8 \pm 0.3	87.9 \pm 0.0	67.3 \pm 2.5	76.7 \pm 0.2
	rank=1	98.5 \pm 0.0	99.2 \pm 0.1	97.4 \pm 0.1	98.5 \pm 0.2	83.5 \pm 0.2	87.0 \pm 0.1	50.0 \pm 3.2	71.0 \pm 0.4
Rank-1 + Quantizer	5 bits	98.5 \pm 0.0	99.2 \pm 0.0	97.2 \pm 0.4	98.5 \pm 0.2	83.4 \pm 0.5	87.0 \pm 0.1	49.6 \pm 3.4	71.6 \pm 0.9
	4 bits	98.6 \pm 0.1	99.2 \pm 0.0	97.4 \pm 0.1	98.6 \pm 0.0	83.6 \pm 0.3	87.0 \pm 0.0	48.1 \pm 3.4	71.3 \pm 0.6
	3 bits	98.6 \pm 0.1	99.2 \pm 0.0	97.3 \pm 0.2	98.6 \pm 0.0	83.7 \pm 0.2	87.0 \pm 0.2	44.7 \pm 3.1	70.3 \pm 0.7

TABLE II: Accuracy for CAFE and Direct compression (CIFAR-10, CIFAR-100).

Compressor	Param.	CIFAR-10 (CONV6, 200 rounds)				CIFAR-100 (ResNet-20, 200 rounds)			
		iid 10 classes/client		non-iid 4 classes/client		iid 100 classes/client		non-iid 40 classes/client	
		Direct	CAFe	Direct	CAFe	Direct	CAFe	Direct	CAFe
None	—	88.5 \pm 0.3		84.4 \pm 0.3		41.3 \pm 1.6		39.3 \pm 1.3	
Top-k	k=10%	86.3 \pm 0.2	87.5 \pm 0.5	81.5 \pm 1.0	83.9 \pm 0.6	33.1 \pm 0.8	37.0 \pm 0.4	32.1 \pm 1.0	34.4 \pm 2.3
	k=1%	74.1 \pm 0.7	80.5 \pm 0.8	70.3 \pm 0.3	76.8 \pm 0.6	19.8 \pm 0.8	23.1 \pm 0.7	19.9 \pm 0.4	21.7 \pm 2.0
	k=0.1%	52.9 \pm 1.6	61.9 \pm 2.4	48.2 \pm 1.5	60.8 \pm 2.8	12.1 \pm 0.7	12.3 \pm 1.2	11.0 \pm 0.4	10.7 \pm 0.3
Top-1% + Quantizer	6 bits	74.5 \pm 0.8	77.5 \pm 1.5	69.4 \pm 1.4	77.0 \pm 0.9	20.1 \pm 0.1	23.4 \pm 1.2	20.0 \pm 0.6	22.0 \pm 0.5
	5 bits	72.9 \pm 0.3	75.3 \pm 0.6	69.7 \pm 2.1	76.5 \pm 1.1	20.0 \pm 0.8	24.0 \pm 0.5	20.7 \pm 0.7	22.0 \pm 0.7
	4 bits	13.1 \pm 2.7	72.5 \pm 2.0	69.2 \pm 0.3	77.0 \pm 0.9	20.7 \pm 0.0	24.3 \pm 0.2	19.1 \pm 0.7	21.7 \pm 0.4
Low-rank	rank=3	65.0 \pm 0.4	80.8 \pm 0.4	62.7 \pm 0.9	76.0 \pm 0.8	19.3 \pm 0.3	32.4 \pm 0.5	19.5 \pm 0.7	26.6 \pm 0.6
	rank=2	59.9 \pm 1.2	78.2 \pm 0.1	57.0 \pm 0.7	72.8 \pm 1.1	16.5 \pm 1.2	29.8 \pm 0.2	17.4 \pm 0.2	24.6 \pm 1.0
	rank=1	53.6 \pm 1.9	72.2 \pm 0.4	45.8 \pm 2.6	62.2 \pm 2.4	12.9 \pm 0.5	24.1 \pm 0.6	13.3 \pm 0.8	17.6 \pm 1.2
Rank-1 + Quantizer	5 bits	52.5 \pm 0.8	71.8 \pm 0.4	43.6 \pm 1.4	62.8 \pm 1.8	13.1 \pm 0.7	24.3 \pm 0.5	12.2 \pm 0.3	17.4 \pm 0.9
	4 bits	53.5 \pm 1.4	70.7 \pm 0.5	46.2 \pm 2.3	62.7 \pm 0.9	13.2 \pm 0.2	23.5 \pm 0.7	14.0 \pm 0.5	16.5 \pm 1.1
	3 bits	53.6 \pm 1.7	68.4 \pm 0.7	44.1 \pm 1.5	61.7 \pm 1.4	13.4 \pm 0.3	22.6 \pm 0.8	13.6 \pm 1.1	17.3 \pm 0.7

TABLE III: Communication cost (Bits Per Parameter) for CAFE and Direct compression (MNIST, EMNIST).

Compressor	Param.	MNIST (CONV4, 50 rounds)				EMNIST (CONV4, 50 rounds)			
		iid 10 classes/client		non-iid 4 classes/client		iid 47 classes/client		non-iid 4 classes/client	
		Direct	CAFe	Direct	CAFe	Direct	CAFe	Direct	CAFe
None	—	$3.20 \cdot 10^1$		$3.20 \cdot 10^1$		$3.20 \cdot 10^1$		$3.20 \cdot 10^1$	
Top-k	k=10%	$5.40 \cdot 10^0$	$5.40 \cdot 10^0$	$5.40 \cdot 10^0$	$5.40 \cdot 10^0$	$5.40 \cdot 10^0$	$5.40 \cdot 10^0$	$5.40 \cdot 10^0$	$5.40 \cdot 10^0$
	k=1%	$5.40 \cdot 10^{-1}$	$5.40 \cdot 10^{-1}$	$5.40 \cdot 10^{-1}$	$5.40 \cdot 10^{-1}$	$5.40 \cdot 10^{-1}$	$5.40 \cdot 10^{-1}$	$5.40 \cdot 10^{-1}$	$5.40 \cdot 10^{-1}$
	k=0.1%	$5.40 \cdot 10^{-2}$	$5.40 \cdot 10^{-2}$	$5.40 \cdot 10^{-2}$	$5.40 \cdot 10^{-2}$	$5.40 \cdot 10^{-2}$	$5.40 \cdot 10^{-2}$	$5.40 \cdot 10^{-2}$	$5.40 \cdot 10^{-2}$
Top-1% + Quantizer	6 bits	$2.80 \cdot 10^{-1}$	$2.80 \cdot 10^{-1}$	$2.77 \cdot 10^{-1}$	$2.76 \cdot 10^{-1}$	$2.80 \cdot 10^{-1}$	$2.80 \cdot 10^{-1}$	$2.76 \cdot 10^{-1}$	$2.78 \cdot 10^{-1}$
	5 bits	$2.66 \cdot 10^{-1}$	$2.64 \cdot 10^{-1}$	$2.55 \cdot 10^{-1}$	$2.59 \cdot 10^{-1}$	$2.68 \cdot 10^{-1}$	$2.68 \cdot 10^{-1}$	$2.46 \cdot 10^{-1}$	$2.55 \cdot 10^{-1}$
	4 bits	$1.96 \cdot 10^{-1}$	$2.55 \cdot 10^{-1}$	$1.38 \cdot 10^{-1}$	$2.13 \cdot 10^{-1}$	$2.47 \cdot 10^{-1}$	$2.51 \cdot 10^{-1}$	$1.57 \cdot 10^{-1}$	$1.83 \cdot 10^{-1}$
Low-rank	rank=3	$4.79 \cdot 10^{-1}$	$4.79 \cdot 10^{-1}$	$4.79 \cdot 10^{-1}$	$4.79 \cdot 10^{-1}$	$4.80 \cdot 10^{-1}$	$4.80 \cdot 10^{-1}$	$4.80 \cdot 10^{-1}$	$4.80 \cdot 10^{-1}$
	rank=2	$3.22 \cdot 10^{-1}$	$3.22 \cdot 10^{-1}$	$3.22 \cdot 10^{-1}$	$3.22 \cdot 10^{-1}$	$3.22 \cdot 10^{-1}$	$3.22 \cdot 10^{-1}$	$3.22 \cdot 10^{-1}$	$3.22 \cdot 10^{-1}$
	rank=1	$1.64 \cdot 10^{-1}$	$1.64 \cdot 10^{-1}$	$1.64 \cdot 10^{-1}$	$1.64 \cdot 10^{-1}$	$1.65 \cdot 10^{-1}$	$1.65 \cdot 10^{-1}$	$1.65 \cdot 10^{-1}$	$1.65 \cdot 10^{-1}$
Rank-1 + Quantizer	5 bits	$2.59 \cdot 10^{-2}$	$2.59 \cdot 10^{-2}$	$2.59 \cdot 10^{-2}$	$2.59 \cdot 10^{-2}$	$2.60 \cdot 10^{-2}$	$2.60 \cdot 10^{-2}$	$2.60 \cdot 10^{-2}$	$2.60 \cdot 10^{-2}$
	4 bits	$2.08 \cdot 10^{-2}$	$2.08 \cdot 10^{-2}$	$2.08 \cdot 10^{-2}$	$2.08 \cdot 10^{-2}$	$2.08 \cdot 10^{-2}$	$2.08 \cdot 10^{-2}$	$2.08 \cdot 10^{-2}$	$2.08 \cdot 10^{-2}$
	3 bits	$1.56 \cdot 10^{-2}$	$1.56 \cdot 10^{-2}$	$1.56 \cdot 10^{-2}$	$1.56 \cdot 10^{-2}$	$1.57 \cdot 10^{-2}$	$1.57 \cdot 10^{-2}$	$1.57 \cdot 10^{-2}$	$1.57 \cdot 10^{-2}$

rank compression on CIFAR-10 (non-iid), CAFE improves accuracy from 45.8% to 62.2%. We plot the learning curves

using Low-rank compression in Fig. 2 to provide a visual comparison of convergence speed and accuracy.

TABLE IV: Communication cost (Bits Per Parameter) for **CAF**e and Direct compression (CIFAR-10, CIFAR-100).

Compressor	Param.	CIFAR-10 (CONV6, 200 rounds)				CIFAR-100 (ResNet-20, 200 rounds)			
		iid		non-iid		iid		non-iid	
		10 classes/client	CAFe	4 classes/client	CAFe	100 classes/client	CAFe	40 classes/client	CAFe
None	—	$3.20 \cdot 10^1$		$3.20 \cdot 10^1$		$3.20 \cdot 10^1$		$3.20 \cdot 10^1$	
Top-k	$k=10\%$	$5.40 \cdot 10^0$	$5.40 \cdot 10^0$	$5.40 \cdot 10^0$	$5.40 \cdot 10^0$	$5.10 \cdot 10^0$	$5.10 \cdot 10^0$	$5.10 \cdot 10^0$	$5.10 \cdot 10^0$
	$k=1\%$	$5.40 \cdot 10^{-1}$	$5.40 \cdot 10^{-1}$	$5.40 \cdot 10^{-1}$	$5.40 \cdot 10^{-1}$	$5.10 \cdot 10^{-1}$	$5.10 \cdot 10^{-1}$	$5.10 \cdot 10^{-1}$	$5.10 \cdot 10^{-1}$
	$k=0.1\%$	$5.40 \cdot 10^{-2}$	$5.40 \cdot 10^{-2}$	$5.40 \cdot 10^{-2}$	$5.40 \cdot 10^{-2}$	$5.11 \cdot 10^{-2}$	$5.11 \cdot 10^{-2}$	$5.11 \cdot 10^{-2}$	$5.11 \cdot 10^{-2}$
Top-1% + Quantizer	6 bits	$2.59 \cdot 10^{-1}$	$2.17 \cdot 10^{-1}$	$2.71 \cdot 10^{-1}$	$2.75 \cdot 10^{-1}$	$2.50 \cdot 10^{-1}$	$2.50 \cdot 10^{-1}$	$2.49 \cdot 10^{-1}$	$2.48 \cdot 10^{-1}$
	5 bits	$2.40 \cdot 10^{-1}$	$2.41 \cdot 10^{-1}$	$2.30 \cdot 10^{-1}$	$2.57 \cdot 10^{-1}$	$2.38 \cdot 10^{-1}$	$2.40 \cdot 10^{-1}$	$1.91 \cdot 10^{-1}$	$2.12 \cdot 10^{-1}$
	4 bits	$6.60 \cdot 10^{-4}$	$1.64 \cdot 10^{-1}$	$1.88 \cdot 10^{-1}$	$2.08 \cdot 10^{-1}$	$2.21 \cdot 10^{-1}$	$2.22 \cdot 10^{-1}$	$1.07 \cdot 10^{-1}$	$1.74 \cdot 10^{-1}$
Low-rank	rank=3	$5.21 \cdot 10^{-1}$	$5.21 \cdot 10^{-1}$	$5.21 \cdot 10^{-1}$	$5.21 \cdot 10^{-1}$	$2.43 \cdot 10^0$	$2.43 \cdot 10^0$	$2.43 \cdot 10^0$	$2.43 \cdot 10^0$
	rank=2	$3.54 \cdot 10^{-1}$	$3.54 \cdot 10^{-1}$	$3.54 \cdot 10^{-1}$	$3.54 \cdot 10^{-1}$	$1.68 \cdot 10^0$	$1.68 \cdot 10^0$	$1.68 \cdot 10^0$	$1.68 \cdot 10^0$
	rank=1	$1.87 \cdot 10^{-1}$	$1.87 \cdot 10^{-1}$	$1.87 \cdot 10^{-1}$	$1.87 \cdot 10^{-1}$	$9.26 \cdot 10^{-1}$	$9.26 \cdot 10^{-1}$	$9.26 \cdot 10^{-1}$	$9.26 \cdot 10^{-1}$
Rank-1 + Quantizer	5 bits	$2.96 \cdot 10^{-2}$	$2.96 \cdot 10^{-2}$	$2.96 \cdot 10^{-2}$	$2.96 \cdot 10^{-2}$	$1.54 \cdot 10^{-1}$	$1.54 \cdot 10^{-1}$	$1.54 \cdot 10^{-1}$	$1.54 \cdot 10^{-1}$
	4 bits	$2.38 \cdot 10^{-2}$	$2.38 \cdot 10^{-2}$	$2.38 \cdot 10^{-2}$	$2.38 \cdot 10^{-2}$	$1.25 \cdot 10^{-1}$	$1.25 \cdot 10^{-1}$	$1.25 \cdot 10^{-1}$	$1.25 \cdot 10^{-1}$
	3 bits	$1.79 \cdot 10^{-2}$	$1.79 \cdot 10^{-2}$	$1.79 \cdot 10^{-2}$	$1.79 \cdot 10^{-2}$	$9.59 \cdot 10^{-2}$	$9.59 \cdot 10^{-2}$	$9.59 \cdot 10^{-2}$	$9.59 \cdot 10^{-2}$

D. Validation of **CAF**e-S

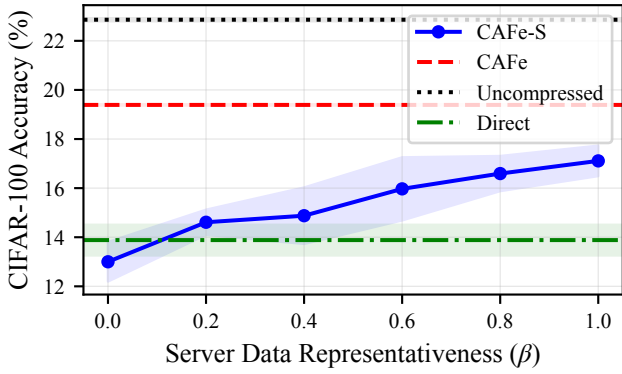


Fig. 3: Accuracy of **CAF**e-S as a function of server’s data representativeness (β) on CIFAR-100. While **CAF**e-S improves as the server’s data become more representative, **CAF**e remains superior due to the stability of the aggregated predictor.

To validate our second proposed framework, **CAF**e-S, we designed an experiment to test the hypothesis of Theorem 3: that the convergence rate depends on the server-client dissimilarity, G^2 . We designed a sensitivity experiment using CIFAR-100. Note that CIFAR-100 is an image classification dataset that has 100 classes grouped into 20 superclasses, making it suitable for creating related but distinct data distributions.

Clients received data from superclasses 0–9. We then created a server-side dataset and tuned its “representativeness” using a parameter $\beta \in [0, 1]$. For $\beta = 1.0$, the server’s data were drawn entirely from superclasses 0–9 (the same as the clients), which makes the server a good proxy for the clients’ data distribution ($G^2 \approx 0$). For $\beta = 0.0$, the server’s data were drawn entirely from superclasses 10–19, which makes the server a non-representative proxy. For $\beta \in (0, 1)$, the server’s data were drawn from both

superclasses, creating a mixed proxy. In all cases, the server’s dataset size was fixed at 10% of the total data.

We plot the accuracy of **CAF**e-S with rank-3 approximation compression against β in Fig. 3, with horizontal baselines corresponding to the **CAF**e and uncompressed methods. As predicted by our theory, the performance of **CAF**e-S improves monotonically as the server’s data become more representative (increasing β). However, we observe that **CAF**e outperforms **CAF**e-S even when $\beta = 1.0$. This reveals a trade-off between *staleness* and *variance*. Although the **CAF**e-S predictor Δ_c^k is “fresh” (computed at Round k), it is generated from a small server split (10% of the total data), leading to higher variance. In contrast, the **CAF**e predictor Δ_s^{k-1} is “stale” (from Round $k-1$), but is aggregated over all clients (90% of the data), making it a significantly more stable estimator of the global gradient direction. This result suggests that while **CAF**e-S effectively leverages server’s data, its advantage over the data-free **CAF**e is conditional on having a large enough dataset at the server to reduce variance below that of the aggregated history.

VI. CONCLUSION

We proposed two novel frameworks, **CAF**e and **CAF**e-S, to improve the efficiency of biased communication compression in distributed learning without relying on stateful clients or per-client error tracking. **CAF**e leverages the previous global update as a shared predictor, making client updates more compressible. **CAF**e-S extends this concept by using a candidate update generated from a server-side dataset, which can serve as a more accurate predictor. We provided convergence guarantees for both methods in the non-convex setting, highlighting a trade-off between the data-free convergence improvement of **CAF**e and the potentially faster convergence of **CAF**e-S, which leverages a representative server-side dataset to mitigate the impact of inter-client heterogeneity. Our experimental results for **CAF**e confirmed its practicality, showing significant im-

provements in convergence speed and model accuracy over standard compressed methods.

APPENDIX A EXPERIMENTAL DETAILS

Our experimental setup, including model architectures, best learning rate per scenario, and data distribution, is summarized in Tables V and VI.

A. Compression Parameter Details

As reported in Tables I and II, we select $k = 10\%$, 1% , and 0.1% for Top-k methods. We also choose uniform quantization with 4, 5, and 6 bits for Top-k + Quantization and uniform quantization with 3, 4, and 5 bits for Low-rank approximation + Quantization. For our Quantization experiments, we fix k to 1% for Top-k and rank to 1 for Low-rank approximation. For Top-k + Quantization compression, we aim to test the lower limit of the choice for the number of bits per coordinate. Notice in Tables I and II that when the number of bits is 4, Direct compression results in performance collapse on CIFAR-10, whereas **CAFe** maintains robustness. For Low-rank compression, **CAFe** consistently outperforms direct compression by a large margin, regardless of the model architecture and dataset. This is due to Low-rank approximation's low compression error, even when using rank 1. With Low-rank approximation + Quantization, we also test the lower limit and find that **CAFe** allows for aggressive quantization (down to 3 bits) where Direct compression typically degrades.

B. Learning Rate Sensitivity

Tables V and VI hints that both **CAFe** and direct compression tend to select similar learning rates. In this section, we provide an ablation study on its sensitivity to the learning rate. Theorem 2 requires a stricter learning rate condition $\gamma \leq \frac{1-\omega}{L(1+\omega)}$ compared to DCGD's $\gamma \leq \frac{1}{L}$. In Fig. 4, we plot the accuracy of both methods on CIFAR-10 (iid) as a function of the learning rate γ . Using direct compression or **CAFe**, we find that both methods have similar performance curve shapes across a range of learning rates, albeit **CAFe**'s is always on top. This suggests that the stricter theoretical bound, required for the Lyapunov proof, may not reflect the practical reality, and **CAFe** does not impose an additional hyperparameter tuning burden.

APPENDIX B PROOFS OF CONVERGENCE THEOREMS

We now present the detailed proofs for the convergence theorems stated in Section IV, restated for clarity. All three convergence proofs analyze the iterates of the form $x^{k+1} = x^k + \Delta_s^k$. We first establish a common notation. Let the local update be

$$\Delta_n^k = -\gamma \nabla f_n(x^k) \quad (12)$$

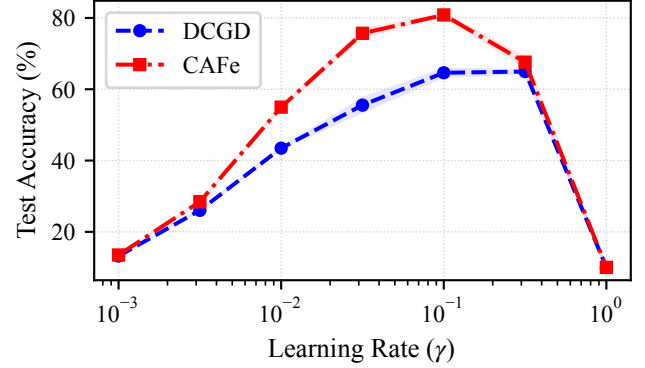


Fig. 4: Learning rate sensitivity analysis on CIFAR-10 (iid) with rank-3 low-rank approximation compression. Both approaches achieve optimal performance around $\gamma = 10^{-1}$ and $\gamma = 10^{-0.5}$ and show similar shapes, suggesting the stricter theoretical bound for **CAFe** may not be a practical limitation.

and the server's candidate update (for **CAFe-S**) be

$$\Delta_c^k = -\gamma \nabla f_s(x^k). \quad (13)$$

The compression error for a client n at step k is e_n^k , and the re-scaled error is $\hat{e}_n^k = e_n^k/\gamma$. The average re-scaled error is $\bar{e}^k = \frac{1}{N} \sum_n \hat{e}_n^k$. Then, the aggregate update Δ_s^k can always be written as:

$$\Delta_s^k = \frac{1}{N} \sum_n (\Delta_n^k + e_n^k) = -\gamma \nabla f(x^k) + \gamma \bar{e}^k.$$

This gives the unified iteration for all algorithms:

$$x^{k+1} = x^k + \Delta_s^k = x^k - \gamma (\nabla f(x^k) - \bar{e}^k). \quad (14)$$

We define the effective gradient as $g^k := \nabla f(x^k) - \bar{e}^k$, so the iteration is $x^{k+1} = x^k - \gamma g^k$.

All proofs start from the standard descent lemma, which follows from Assumption 1 and a learning rate $\gamma \leq \frac{1}{L}$:

$$\begin{aligned} f(x^{k+1}) &\leq f(x^k) + \langle \nabla f(x^k), x^{k+1} - x^k \rangle + \frac{L}{2} \|x^{k+1} - x^k\|^2 \\ &= f(x^k) - \gamma \langle \nabla f(x^k), g^k \rangle + \frac{L\gamma^2}{2} \|g^k\|^2 \\ &\leq f(x^k) - \frac{\gamma}{2} \|\nabla f(x^k)\|^2 - \left(\frac{\gamma}{2} - \frac{L\gamma^2}{2} \right) \|g^k\|^2 \\ &\quad + \frac{\gamma}{2} \|\nabla f(x^k) - g^k\|^2 \end{aligned} \quad (15)$$

$$\leq f(x^k) - \frac{\gamma}{2} \|\nabla f(x^k)\|^2 + \frac{\gamma}{2} \|\bar{e}^k\|^2. \quad (16)$$

The final inequality holds for $\gamma \leq \frac{1}{L}$ (which makes the $\|g^k\|^2$ term negative) and uses $\|\nabla f(x^k) - g^k\|^2 = \|\nabla f(x^k) - (\nabla f(x^k) - \bar{e}^k)\|^2 = \|\bar{e}^k\|^2$. The proofs for the three theorems differ only in how they bound the $\mathbb{E} [\|\bar{e}^k\|^2]$ term.

TABLE V: Optimal learning rates for CAFE and Direct compression (MNIST, EMNIST).

Compressor	Param.	MNIST (CONV4, 50 rounds)				EMNIST (CONV4, 50 rounds)			
		iid		non-iid		iid		non-iid	
		10 classes/client	CAFe	4 classes/client	CAFe	47 classes/client	CAFe	4 classes/client	CAFe
None	—	$10^{-0.5}$		0.1		$10^{-0.5}$		0.1	
Top-k	k=10%	$10^{-0.5}$	$10^{-0.5}$	$10^{-0.5}$	0.1	$10^{-0.5}$	$10^{-0.5}$	0.1	0.1
	k=1%	$10^{-0.5}$	$10^{-0.5}$	0.1	0.1	$10^{-0.5}$	$10^{-0.5}$	0.1	0.1
	k=0.1%	0.1	0.1	$10^{-0.5}$	0.1	0.1	0.1	0.1	0.1
Top-1% + Quantizer	6 bits	$10^{-0.5}$	$10^{-0.5}$	0.1	0.1	$10^{-0.5}$	$10^{-0.5}$	0.1	0.1
	5 bits	$10^{-0.5}$	$10^{-0.5}$	0.1	0.1	$10^{-0.5}$	$10^{-0.5}$	$10^{-0.5}$	0.1
	4 bits	$10^{-0.5}$	0.1	0.1	0.1	$10^{-0.5}$	$10^{-0.5}$	0.1	0.1
Low-rank	rank=3	0.1	$10^{-0.5}$	0.1	0.1	0.1	0.1	0.1	0.1
	rank=2	0.1	0.1	0.1	0.1	$10^{-0.5}$	0.1	$10^{-1.5}$	$10^{-1.5}$
	rank=1	0.1	0.1	0.1	0.1	0.1	0.1	$10^{-1.5}$	$10^{-1.5}$
Rank-1 + Quantizer	5 bits	0.1	0.1	0.1	0.1	0.1	0.1	$10^{-1.5}$	$10^{-1.5}$
	4 bits	0.1	0.1	0.1	0.1	0.1	0.1	$10^{-1.5}$	$10^{-1.5}$
	3 bits	0.1	0.1	0.1	0.1	0.1	0.1	$10^{-1.5}$	$10^{-1.5}$

TABLE VI: Optimal learning rates for CAFE and Direct compression (CIFAR-10, CIFAR-100).

Compressor	Param.	CIFAR-10 (CONV6, 200 rounds)				CIFAR-100 (ResNet-20, 200 rounds)			
		iid		non-iid		iid		non-iid	
		10 classes/client	CAFe	4 classes/client	CAFe	100 classes/client	CAFe	40 classes/client	CAFe
None	—	$10^{-0.5}$		0.1		$10^{-0.5}$		1	
Top-k	k=10%	$10^{-0.5}$	0.1	$10^{-0.5}$	0.1	$10^{-0.5}$	$10^{-0.5}$	1	1
	k=1%	$10^{-0.5}$	0.1	$10^{-0.5}$	0.1	1	$10^{-0.5}$	1	1
	k=0.1%	$10^{-0.5}$	0.1	0.1	0.1	1	0.1	1	$10^{-0.5}$
Top-1% + Quantizer	6 bits	$10^{-0.5}$	0.1	$10^{-0.5}$	0.1	$10^{-0.5}$	1	1	1
	5 bits	$10^{-0.5}$	$10^{-0.5}$	$10^{-0.5}$	0.1	1	$10^{-0.5}$	1	1
	4 bits	0.01	$10^{-0.5}$	0.1	0.1	$10^{-0.5}$	$10^{-0.5}$	1	$10^{-0.5}$
Low-rank	rank=3	$10^{-0.5}$	0.1	0.1	0.1	$10^{-0.5}$	$10^{-0.5}$	1	$10^{-0.5}$
	rank=2	0.1	0.1	0.1	0.1	$10^{-0.5}$	$10^{-0.5}$	1	$10^{-0.5}$
	rank=1	$10^{-0.5}$	0.1	0.1	0.1	$10^{-0.5}$	$10^{-0.5}$	1	$10^{-0.5}$
Rank-1 + Quantizer	5 bits	$10^{-0.5}$	0.1	0.1	0.1	$10^{-0.5}$	$10^{-0.5}$	1	$10^{-0.5}$
	4 bits	$10^{-0.5}$	0.1	$10^{-0.5}$	0.1	$10^{-0.5}$	$10^{-0.5}$	1	$10^{-0.5}$
	3 bits	0.1	0.1	0.1	$10^{-1.5}$	$10^{-0.5}$	0.1	1	$10^{-0.5}$

A. Proof of Theorem 1 (DCGD)

Jensen's inequality

$$\begin{aligned}
\mathbb{E} [\|\bar{e}^k\|^2] &= \mathbb{E} \left[\left\| \frac{1}{N} \sum_n \hat{e}_n^k \right\|^2 \right] \leq \frac{1}{N} \sum_n \mathbb{E} [\|\hat{e}_n^k\|^2] \\
&= \frac{1}{N\gamma^2} \sum_n \mathbb{E} [\|e_n^k\|^2] \\
&\leq \frac{\omega}{N\gamma^2} \sum_n \mathbb{E} [\|\Delta_n^k\|^2] \quad (\text{by Eq. (2)}) \\
&= \omega \frac{1}{N} \sum_n \mathbb{E} [\|\nabla f_n(x^k)\|^2] \\
&\leq \omega B^2 \mathbb{E} [\|\nabla f(x^k)\|^2]. \quad (\text{by Assumption 2})
\end{aligned}$$

Theorem 1. [DCGD Convergence] Under Assumptions 1 and 2, with a learning rate $\gamma \leq \frac{1}{L}$ and a compression parameter ω such that $\omega B^2 < 1$, DCGD satisfies

$$\frac{1}{K} \sum_{k=0}^{K-1} \mathbb{E} [\|\nabla f(x^k)\|^2] \leq \frac{2(f(x^0) - f^*)}{\gamma K} \cdot \frac{1}{1 - \omega B^2}. \quad (6)$$

Proof. For standard DCGD (Algorithm 1), clients compress their raw local update Δ_n^k . The error is $e_n^k = \mathcal{C}(\Delta_n^k) - \Delta_n^k$. We bound the expectation of its squared norm using

$$\begin{aligned}
\mathbb{E} [f(x^{k+1})] &\leq \mathbb{E} \left[f(x^k) - \frac{\gamma}{2} \|\nabla f(x^k)\|^2 + \frac{\gamma}{2} \|\bar{e}^k\|^2 \right] \\
&= \mathbb{E} [f(x^k)] - \frac{\gamma}{2} (1 - \omega B^2) \mathbb{E} [\|\nabla f(x^k)\|^2].
\end{aligned}$$

Next, we substitute this error bound into our descent lemma (Eq. (16)) and take the expectation:

Re-arranging and telescoping this from $k = 0$ to $K - 1$ yields

$$\begin{aligned} \frac{\gamma}{2}(1 - \omega B^2) \sum_{k=0}^{K-1} \mathbb{E} \left[\|\nabla f(x^k)\|^2 \right] &\leq f(x^0) - \mathbb{E} [f(x^K)] \\ &\leq f(x^0) - f^*. \end{aligned}$$

Dividing by K and re-arranging gives the theorem's statement. \square

B. Proof of Theorem 2 (CAF ϵ)

The proof for CAF ϵ is more complex as the error \bar{e}^k depends on the previous update Δ_s^{k-1} , which itself contains \bar{e}^{k-1} . This requires a Lyapunov analysis. We first need three supporting lemmas.

Lemma 3. *Given an L -smooth function f , and iterations of the form $x^{k+1} = x^k - \gamma g^k$, we have*

$$-\langle \nabla f(x^{k+1}), g^k \rangle \leq -\langle \nabla f(x^k), g^k \rangle + \gamma L \|g^k\|^2. \quad (17)$$

Proof. We have

$$\begin{aligned} -\langle \nabla f(x^{k+1}), g^k \rangle &= -\langle \nabla f(x^k), g^k \rangle \\ &\quad + \langle \nabla f(x^k) - \nabla f(x^{k+1}), g^k \rangle, \end{aligned}$$

and this can be bounded by

$$\begin{aligned} \langle \nabla f(x^{k+1}) - \nabla f(x^k), g^k \rangle &\leq \|\nabla f(x^{k+1}) - \nabla f(x^k)\| \|g^k\| \\ &\leq \gamma L \|g^k\|^2, \end{aligned}$$

where we have used the L -smoothness of f in the last step. Re-arranging, we obtain the desired result. \square

Lemma 4. *Given Assumptions 1 and 2, the compression error for DGD + CAF ϵ (with $g^k = \nabla f(x^k) - \bar{e}^k$) satisfies*

$$\begin{aligned} \mathbb{E} \left[\|\bar{e}^{k+1}\|^2 \right] &\leq \omega \mathbb{E} \left[B^2 \|\nabla f(x^{k+1})\|^2 - \|\nabla f(x^k)\|^2 \right] \\ &\quad + \gamma 2\omega L \mathbb{E} \left[\|g^k\|^2 \right] + \omega \mathbb{E} \left[\|\bar{e}^k\|^2 \right]. \end{aligned} \quad (18)$$

Proof. We start by bounding the next-step error:

$$\begin{aligned} \mathbb{E} \left[\|\bar{e}^{k+1}\|^2 \right] &\leq \frac{1}{N} \sum_n \mathbb{E} \left[\|\hat{e}_n^{k+1}\|^2 \right] \quad (\text{by Jensen's}) \\ &= \frac{1}{N\gamma^2} \sum_n \mathbb{E} \left[\|e_n^{k+1}\|^2 \right] \end{aligned}$$

In CAF ϵ , clients compress $(\Delta_n^{k+1} - \Delta_s^k)$. So, by Eq. (2), the last is upper bounded by

$$\begin{aligned} &\frac{\omega}{N\gamma^2} \sum_n \mathbb{E} \left[\|\Delta_n^{k+1} - \Delta_s^k\|^2 \right] \\ &= \frac{\omega}{N\gamma^2} \sum_n \mathbb{E} \left[\|-\gamma \nabla f_n(x^{k+1}) - (-\gamma g^k)\|^2 \right] \\ &= \frac{\omega}{N} \sum_n \mathbb{E} \left[\|\nabla f_n(x^{k+1}) - g^k\|^2 \right]. \end{aligned}$$

We add and subtract $\nabla f(x^{k+1})$ inside the norm, and expand. Note that the cross-terms $\langle \nabla f_n - \nabla f, \nabla f - g^k \rangle$ sum over n is zero, so the last expression equals

$$\begin{aligned} \omega \mathbb{E} \left[\frac{1}{N} \sum_n \|\nabla f_n(x^{k+1}) - \nabla f(x^{k+1})\|^2 \right] \\ + \omega \mathbb{E} \left[\|\nabla f(x^{k+1}) - g^k\|^2 \right] \end{aligned} \quad (19)$$

Using Assumption 2 we can bound the first term in Eq. (19) as

$$\begin{aligned} \frac{1}{N} \sum_n \|\nabla f_n - \nabla f\|^2 &= \left(\frac{1}{N} \sum_n \|\nabla f_n\|^2 \right) - \|\nabla f\|^2 \\ &\leq (B^2 - 1) \|\nabla f\|^2. \end{aligned}$$

Thus, to finish we expand the last term in Eq. (19),

$$\begin{aligned} \|\nabla f(x^{k+1}) - g^k\|^2 &= \|\nabla f(x^{k+1})\|^2 + \|g^k\|^2 \\ &\quad - 2 \langle \nabla f(x^{k+1}), g^k \rangle, \end{aligned}$$

and apply Lemma 3 to bound the inner product term. This gives us

$$\begin{aligned} \|\nabla f(x^{k+1}) - g^k\|^2 &\leq \left(\|\nabla f(x^{k+1})\|^2 - \|\nabla f(x^k)\|^2 \right) \\ &\quad + \left(\|\nabla f(x^k)\|^2 - 2 \langle \nabla f(x^k), g^k \rangle + \|g^k\|^2 \right) \\ &\quad + 2\gamma L \|g^k\|^2 \end{aligned}$$

The middle term is $\|\nabla f(x^k) - g^k\|^2 = \|\bar{e}^k\|^2$, so plugging this back into our main inequality gives the lemma. \square

Lemma 5. *Let $f: \mathbb{R}^d \rightarrow \mathbb{R}$ be an L -smooth function with a lower bound f^* . Then, for any $x \in \mathbb{R}^d$,*

$$\|\nabla f(x)\|^2 \leq 2L(f(x) - f^*).$$

Proof. By Assumption 1, for any y , we have

$$f(y) \leq f(x) + \langle \nabla f(x), y - x \rangle + \frac{L}{2} \|y - x\|^2.$$

We choose $y = x - \frac{1}{L} \nabla f(x)$, and obtain

$$f(y) \leq f(x) - \frac{1}{2L} \|\nabla f(x)\|^2.$$

Since $f(y) \geq f^*$, we re-arrange and obtain the result. \square

Theorem 2. [CAF ϵ + DGD Convergence] *Under Assumptions 1 and 2, with a learning rate*

$$\gamma \leq \frac{1 - \omega}{L(1 + \omega)} \quad (7)$$

and $\omega B^2 < 1$, CAF ϵ with DGD satisfies

$$\frac{1}{K} \sum_{k=0}^{K-1} \mathbb{E} \left[\|\nabla f(x^k)\|^2 \right] \leq \frac{2(f(x^0) - f^*)}{\gamma K} \cdot \frac{1 - \omega}{1 - \omega B^2}. \quad (8)$$

Proof. First, we define a Lyapunov function to capture both the function value and the compression error. Let

$$\Psi^k := \mathbb{E} \left[f(x^k) + \frac{\gamma}{2(1 - \omega)} \|\bar{e}^k\|^2 \right]. \quad (20)$$

Our goal is to show that $\Psi^{k+1} \leq \Psi^k$ – (progress term). We will combine the descent lemma (Eq. (16)) and the compression error bound from Lemma 4. We start with the expectation of the descent lemma (Eq. (15))

$$\begin{aligned}\mathbb{E}[f(x^{k+1})] &\leq \mathbb{E}[f(x^k)] - \frac{\gamma}{2} \mathbb{E}[\|\nabla f(x^k)\|^2] \\ &\quad + \frac{\gamma}{2} \mathbb{E}[\|\bar{e}^k\|^2] \\ &\quad - \left(\frac{1}{2\gamma} - \frac{L}{2}\right) \mathbb{E}[\|x^{k+1} - x^k\|^2]\end{aligned}$$

and $\frac{\gamma}{2(1-\omega)} \cdot \mathbb{E}[\text{Lemma 4}]$, which yields

$$\begin{aligned}\frac{\gamma \mathbb{E}[\|e^{k+1}\|^2]}{2(1-\omega)} &\leq \frac{\gamma \omega \mathbb{E}[\|e^k\|^2]}{2(1-\omega)} \\ &\quad + \frac{\gamma \omega}{2(1-\omega)} \mathbb{E}[B^2 \|\nabla f^{k+1}\|^2 - \|\nabla f^k\|^2] \\ &\quad + \frac{\gamma^2 \omega L}{1-\omega} \mathbb{E}[\|g^k\|^2].\end{aligned}$$

Summing these two inequalities gives

$$\begin{aligned}\Psi^{k+1} &\leq \underbrace{\left(\mathbb{E}[f(x^k)] + \frac{\gamma \omega \mathbb{E}[\|\bar{e}^k\|^2]}{2(1-\omega)} + \frac{\gamma}{2} \mathbb{E}[\|\bar{e}^k\|^2] \right)}_{=\Psi^k} \\ &\quad + \underbrace{\left(-\frac{\gamma}{2} \mathbb{E}[\|\nabla f^k\|^2] - \frac{\gamma \omega}{2(1-\omega)} \mathbb{E}[\|\nabla f^k\|^2] \right)}_{=-\frac{\gamma}{2(1-\omega)} \mathbb{E}[\|\nabla f^k\|^2]} \\ &\quad - \underbrace{\left(\frac{1}{2\gamma} - \frac{L}{2} - \frac{\gamma \omega L}{1-\omega} \right) \mathbb{E}[\|x^{k+1} - x^k\|^2]}_{\leq 0 \text{ by Eq. (7)}} \\ &\quad + \frac{\gamma \omega B^2}{2(1-\omega)} \mathbb{E}[\|\nabla f(x^{k+1})\|^2].\end{aligned}$$

The Ψ^k term simplifies because $\frac{\gamma \omega}{2(1-\omega)} + \frac{\gamma}{2} = \frac{\gamma}{2(1-\omega)}$. The $\|\nabla f^k\|^2$ term simplifies to $-\frac{\gamma(1-\omega)+\gamma\omega}{2(1-\omega)} = -\frac{\gamma}{2(1-\omega)}$. The $\|x^{k+1} - x^k\|^2$ term is negative due to Eq. (7), so we can drop it. Thus,

$$\begin{aligned}\Psi^{k+1} &\leq \Psi^k - \frac{\gamma}{2(1-\omega)} \mathbb{E}[\|\nabla f(x^k)\|^2] \\ &\quad + \frac{\gamma \omega B^2}{2(1-\omega)} \mathbb{E}[\|\nabla f(x^{k+1})\|^2].\end{aligned}$$

Given that $\omega B^2 < 1$, this almost gives us our desired Lyapunov decrease. We have taken the liberty of calling Ψ^k the Lyapunov function, but it does not strictly decrease due to the last term, which depends on the next iterate x^{k+1} , instead of x^k . We will handle the extra term by first telescoping the recursion from $k = 0$ to $K - 1$,

$$\begin{aligned}\Psi^K &\leq \Psi^0 - \frac{\gamma}{2(1-\omega)} \sum_{k=0}^{K-1} \mathbb{E}[\|\nabla f(x^k)\|^2] \\ &\quad + \frac{\gamma \omega B^2}{2(1-\omega)} \sum_{k=0}^{K-1} \mathbb{E}[\|\nabla f(x^{k+1})\|^2].\end{aligned}$$

Given $\Psi^0 = f(x^0)$, since $\bar{e}^0 = 0$, and $\Psi^K \geq f(x^K)$, we obtain

$$\begin{aligned}f(x^K) &\leq f(x^0) - \frac{\gamma(1-\omega B^2)}{2(1-\omega)} \sum_{k=0}^{K-1} \mathbb{E}[\|\nabla f(x^k)\|^2] \\ &\quad + \frac{\gamma \omega B^2}{2(1-\omega)} \mathbb{E}[\|\nabla f(x^K)\|^2],\end{aligned}$$

where we have dropped a negative $\|\nabla f(x^0)\|^2$ term. Next, we use Lemma 5 to bound the $\mathbb{E}[\|\nabla f(x^K)\|^2]$ term,

$$\begin{aligned}\frac{\gamma(1-\omega B^2)}{2(1-\omega)} \sum_{k=0}^{K-1} \mathbb{E}[\|\nabla f(x^k)\|^2] &\leq \\ f(x^0) + \frac{\gamma \omega B^2}{2(1-\omega)} 2L(f(x^K) - f^*) - f(x^K).\end{aligned}$$

To obtain the theorem statement, it suffices to show that

$$\frac{\gamma \omega B^2}{2(1-\omega)} 2L(f(x^K) - f^*) - f(x^K) \leq -f^*, \quad (21)$$

which holds if

$$\frac{\gamma \omega B^2}{1-\omega} L < 1. \quad (22)$$

Notice that this is equivalent to Eq. (7), given that $\omega B^2 < 1$. Thus, we have completed the proof. \square

C. Proof of Theorem 3 (CAFe-S)

Theorem 3. [CAFe-S + DGD Convergence] Under Assumptions 1 to 3, with a learning rate $\gamma \leq \frac{1}{L}$, and a compression parameter ω such that $\omega G^2 B^2 < 1$, CAFe-S with DGD satisfies

$$\frac{1}{K} \sum_{k=0}^{K-1} \mathbb{E}[\|\nabla f(x^k)\|^2] \leq \frac{2(f(x^0) - f^*)}{\gamma K(1 - \omega G^2 B^2)}. \quad (10)$$

Proof. This proof follows the same structure as the DCGD proof. For CAFe-S, clients compress the difference $\Delta_n^k - \Delta_c^k$. The error is $e_n^k = \mathcal{C}(\Delta_n^k - \Delta_c^k) - (\Delta_n^k - \Delta_c^k)$.

$$\begin{aligned}\mathbb{E}[\|\bar{e}^k\|^2] &\leq \frac{1}{N} \sum_n \mathbb{E}[\|\hat{e}_n^k\|^2] \quad \text{(by Jensen's)} \\ &= \frac{1}{N\gamma^2} \sum_n \mathbb{E}[\|e_n^k\|^2] \\ &\leq \frac{\omega}{N\gamma^2} \sum_n \mathbb{E}[\|\Delta_n^k - \Delta_c^k\|^2] \quad \text{(by Eq. (2))} \\ &= \omega \frac{1}{N} \sum_n \mathbb{E}[\|\nabla f_n(x^k) - \nabla f_s(x^k)\|^2] \\ &\leq \omega G^2 \frac{1}{N} \sum_n \mathbb{E}[\|\nabla f_n(x^k)\|^2] \\ &\leq \omega G^2 B^2 \mathbb{E}[\|\nabla f(x^k)\|^2]. \quad \text{(by Assumption 3)}\end{aligned}$$

Now, notice that this error bound has the *exact same form* as the DCGD error bound, with the constant ωB^2 simply replaced by $\omega G^2 B^2$. The remainder of the proof (telescoping the sum and re-arranging) is identical to the proof for Theorem 1. \square

REFERENCES

[1] T. Ortega, C.-Y. Huang, X. Li, and H. Jafarkhani, “Communication compression for distributed learning without control variates,” *arXiv*, no. arXiv:2412.04538, Dec. 2024, arXiv:2412.04538 [cs]. [Online]. Available: <http://arxiv.org/abs/2412.04538>

[2] B. McMahan, E. Moore, D. Ramage, S. Hampson, and B. A. y. Arcas, “Communication-efficient learning of deep networks from decentralized data,” in *Proceedings of the 20th International Conference on Artificial Intelligence and Statistics*. PMLR, 4 2017, pp. 1273–1282. [Online]. Available: <https://proceedings.mlr.press/v54/mcmahan17a.html>

[3] P. Kairouz, H. B. McMahan, B. Avent, A. Bellet, M. Bennis, A. Nitin Bhagoji *et al.*, “Advances and open problems in federated learning,” *Foundations and Trends® in Machine Learning*, vol. 14, no. 1-2, pp. 1–210, 2021. [Online]. Available: <http://www.nowpublishers.com/article/Details/MAL-083>

[4] D. Alistarh, D. Grubic, J. Li, R. Tomioka, and M. Vojnovic, “QSGD: Communication-efficient SGD via gradient quantization and encoding,” in *Advances in Neural Information Processing Systems*, I. Guyon, U. V. Luxburg, S. Bengio, H. Wallach, R. Fergus, S. Vishwanathan, and R. Garnett, Eds., vol. 30. Curran Associates, Inc., 2017. [Online]. Available: <https://proceedings.neurips.cc/paper/2017/file/6c340f25839e6acdc73414517203f5f0-Paper.pdf>

[5] A. Aji and K. Heafield, “Sparse communication for distributed gradient descent,” in *EMNLP 2017: Conference on Empirical Methods in Natural Language Processing*. Association for Computational Linguistics (ACL), 2017.

[6] T. Vogels, S. P. Karimireddy, and M. Jaggi, “PowerSGD: Practical low-rank gradient compression for distributed optimization,” *Advances in Neural Information Processing Systems*, vol. 32, 2019.

[7] A. Beznosikov, S. Horváth, P. Richtárik, and M. Safaryan, “On biased compression for distributed learning,” *Journal of Machine Learning Research*, vol. 24, no. 276, pp. 1–50, 2023.

[8] S. P. Karimireddy, Q. Rebjock, S. Stich, and M. Jaggi, “Error feedback fixes signSGD and other gradient compression schemes,” in *Proceedings of the 36th International Conference on Machine Learning*. PMLR, 5 2019, pp. 3252–3261. [Online]. Available: <https://proceedings.mlr.press/v97/karimireddy19a.html>

[9] A. Reibman, H. Jafarkhani, Y. Wang, M. Orchard, and R. Puri, “Multiple-description video coding using motion-compensated temporal prediction,” *IEEE Transactions on Circuits and Systems for Video Technology*, vol. 12, no. 3, pp. 193–204, 2002.

[10] S. P. Karimireddy, S. Kale, M. Mohri, S. Reddi, S. Stich, and A. T. Suresh, “SCAFFOLD: Stochastic controlled averaging for federated learning,” in *Proceedings of the 37th International Conference on Machine Learning*. PMLR, 11 2020, pp. 5132–5143. [Online]. Available: <https://proceedings.mlr.press/v119/karimireddy20a.html>

[11] S. U. Stich, J.-B. Cordonnier, and M. Jaggi, “Sparsified SGD with memory,” in *Advances in Neural Information Processing Systems*, vol. 31. Curran Associates, Inc., 2018. [Online]. Available: <https://proceedings.neurips.cc/paper/2018/hash/b440509a0106086a67bc2ea9df0a1dab-Abstract.html>

[12] D. Alistarh, T. Hoefler, M. Johansson, N. Konstantinov, S. Khirirat, and C. Renggli, “The convergence of sparsified gradient methods,” in *Advances in Neural Information Processing Systems*, vol. 31. Curran Associates, Inc., 2018. [Online]. Available: https://proceedings.neurips.cc/paper_files/paper/2018/hash/314450613369e0ee72d0da7f6fe773c-Abstract.html

[13] A. Koloskova, S. Stich, and M. Jaggi, “Decentralized stochastic optimization and gossip algorithms with compressed communication,” in *Proceedings of the 36th International Conference on Machine Learning*. PMLR, 5 2019, pp. 3478–3487. [Online]. Available: <https://proceedings.mlr.press/v97/koloskova19a.html>

[14] T. Ortega and H. Jafarkhani, “Gossiped and quantized online multi-kernel learning,” *IEEE Signal Processing Letters*, vol. 30, pp. 468–472, 2023.

[15] ———, “Asynchronous federated learning with bidirectional quantized communications and buffered aggregation,” *arXiv*, no. arXiv:2308.00263, july 2023, arXiv:2308.00263 [cs, eess, math]. [Online]. Available: <http://arxiv.org/abs/2308.00263>

[16] ———, “Quantized and asynchronous federated learning,” *IEEE Transactions on Communications*, vol. 73, no. 4, pp. 2361–2374, 2025.

[17] P. Richtarik, I. Sokolov, and I. Fatkhullin, “EF21: A new, simpler, theoretically better, and practically faster error feedback,” in *Advances in Neural Information Processing Systems*, vol. 34. Curran Associates, Inc., 2021, pp. 4384–4396. [Online]. Available: <https://proceedings.neurips.cc/paper/2021/hash/231141b34c82aa95e48810a9d1b33a79-Abstract.html>

[18] Ookla, “Speedtest global index – internet speed around the world,” <https://www.speedtest.net/global-index>, 2025, accessed: 2025-12-16.

[19] Y. Nesterov, *Lectures on Convex Optimization*, ser. Springer Optimization and Its Applications. Cham: Springer International Publishing, 2018, vol. 137. [Online]. Available: <http://link.springer.com/10.1007/978-3-319-91578-4>

[20] T. Ortega, “CAFe,” <https://github.com/TomasOrtega/CAFe>, 2025.

[21] Y. LeCun, L. Bottou, Y. Bengio, and P. Haffner, “Gradient-based learning applied to document recognition,” *Proceedings of the IEEE*, vol. 86, no. 11, pp. 2278–2324, 1998.

[22] G. Cohen, S. Afshar, J. Tapson, and A. Van Schaik, “EMNIST: Extending mnist to handwritten letters,” in *2017 international joint conference on neural networks (IJCNN)*. IEEE, 2017, pp. 2921–2926.

[23] A. Krizhevsky and G. Hinton, “Learning multiple layers of features from tiny images,” Master’s thesis, Department of Computer Science, University of Toronto, 2009.

[24] B. Isik, F. Pase, D. Gunduz, S. Koyejo, T. Weissman, and M. Zorzi, “Adaptive compression in federated learning via side information,” in *International Conference on Artificial Intelligence and Statistics*. PMLR, 2024, pp. 487–495.

[25] S. B. Harma, A. Chakraborty, E. Kostenok, D. Mishin, D. Ha, B. Falsafi, M. Jaggi, M. Liu, Y. Oh, S. Subramanian *et al.*, “Effective interplay between sparsity and quantization: From theory to practice,” *arXiv preprint arXiv:2405.20935*, 2024.